Dual Drug Release from CO_2-Infused Nanofibers via Hydrophobic and Hydrophilic Interactions

Undergraduate Honors Thesis of:

Brett Geiger, Class of 2014

For Graduation with Honors Research Distinction in Biomedical Engineering from The Ohio State University

Committee: Professors John Lannutti and Heather Powell

Abstract

CO_2 infusion of biomolecules is a benign, green, and inexpensive method to provide much-needed biochemical activity to electrospun nanofibers for tissue engineering applications. This study investigated the effects of hydrophobic-hydrophilic interactions on dual drug release from CO_2-infused nanofibers (PCL, PCL-gelatin, and PCL 'core' PCL-gelatin 'shell') using BODIPY 493/503 and Rhodamine B fluorescent dyes as drug models. Interestingly, when exposed to supercritical CO_2, core-shell fibers did not melt. Positive dye-matrix interactions led to increased dye loading and gradual, linear release. Conversely, the opposite was observed for negative interactions. When two dyes were infused, this behavior was accentuated due to interactions between dyes. CO_2 infusion, without changing scaffold microstructure, positively impacted both dye loading and longer-term release when individual dyes were infused into scaffolds of unlike polarity. Core-shell nanofibers displayed radically different release properties versus PCL-gelatin when treated with dyes via CO_2 infusion. Dye release from core-shell scaffolds was highly sensitive to both interactions with scaffolds and phase of CO_2. By using different phases of CO_2 to partition dyes into hydrophobic and hydrophilic sections of core-shell nanofiber scaffolds, interactions can be manipulated to develop a bimodal drug release system.

Acknowledgements

I would like to thank Professor Lannutti for giving me the opportunity to begin research as a freshman with no prior experience, under the sole condition that I do not break things. My early exposure to science has enabled me to experience far more growth as an undergraduate researcher. I would also like to thank Tyler Nelson for his incredible mentorship over the past 3 years, which has been instrumental in my development as an independent researcher. Finally, I would like to thank the College of Engineering for providing me with funding throughout this project.

This work is supported by a research grant from the National Science Foundation under Grant No. EEC-0425626. Any opinions, findings, and conclusions or recommendations expressed in this material are those of the author and do not necessarily reflect the views of the National Science Foundation or The Ohio State University.

Table of Contents

List of Figures and Tables

1 Introduction

Biomimetic materials, both synthetic and natural, have been applied as wound dressings to accelerate the healing process. In early efforts alginate, a compound derived from seaweed, was used as the basis for wound dressings [1,2]. Other natural polymers including collagen, fibrin, chitosan, and even xenograft dermis have been investigated and utilized for their ability to interact favorably with cells at the wound site and provide a biological microstructure mimicking the extracellular matrix (ECM) of human tissues [3-8]. In contrast, synthetic polymers have a distinct advantage in that they are easily tailored for a specific application, providing an engineered alternative with control over properties such as modulus and degradation rate [9-11]. Biocompatible polymers such as polyglycolic acid (PGA), polylactic acid (PLA), polyurethane (PU), and polycaprolactone (PCL) see widespread use in wound healing and tissue engineering applications [9,12-14]. However, a shortcoming of these synthetic materials lies in their inherently limited biofunctionality. Electrospinning is a polymer processing technique that has been used to produce nano-scale diameter fibers from all of these synthetics, providing a high surface-area substrate resembling the microstructure and morphology of native ECM, which is attractive for regenerative medicine applications [9,12-17]. Bioactivity is often further augmented with methods to incorporate drugs or growth factors.

To further these goals, investigators have applied many different techniques of biofunctionalization to electrospun nanofibers, including adhesion treatments, surface coupling of biomolecules, and drug infusion into the polymer bulk [17-21]. In particular, controlled release of incorporated drugs is an expanding area of research, due to the enormous potential to affect biologic sites via spatiotemporal differences in drug

application [22]. Approaches for control include diffusion barrier manipulation, tailored solvent swelling, chemical degradation, and actuation of external stimuli such as magnetic fields or heat [21]. While in some cases effective, these methods can prove challenging to control and often lead to deleterious effects on nanofiber morphology or drug bioactivity [23]. Supercritical fluids technology utilizes the phase transition of carbon dioxide to provide an effective means of drug incorporation and release from nanofiber scaffolds via precise control of drug impregnation with experimental pressure and temperature of CO_2 [24]. Previous studies have established both supercritical and subcritical CO_2 infusion as benign, green, and inexpensive techniques that can be used to biofunctionalize nanofiber scaffolds [24-26].

In this context, chronic wounds are a specific type of condition that, due to a malfunction in the natural healing process, can take years to heal and in some cases may not heal at all. This results in long term pain, persistent infection, and lengthy hospitalizations [27]. These wounds affect nearly 6.5 million patients in the United States alone, resulting in a yearly medical expenditure of $25 billion [27]. The biological causes of aberrancy in chronic wounds are quite complex. Therefore, recent engineering approaches to scaffold design for this application frequently incorporate multiple drugs into a single scaffold [22,28-31]. Thus, controlled release has become increasingly important as interactions between these drugs as well as interactions between the drugs and scaffold must be elucidated. Hydrophobic-hydrophilic interactions are a factor playing a prominent role in diffusion-based release [21]. Several studies have proposed these interactions as possible causes for observed release behavior but few have investigated and quantified the effect of such interactions on release [29,30,32]. To make

progress toward the goal of an electrospun nanofiber scaffold having multiple drug functionalizations realized by CO_2 infusion, this study aims to investigate the effects that hydrophobic-hydrophilic match and mismatch have on the loading and release of drugs infused into electrospun nanofibers via supercritical or subcritical CO_2 exposure.

Drugs were modeled in this study using two different fluorescent dyes. Rhodamine B ([9-(2-carboxyphenyl)-6-diethylamino-3-xanthenylidene]-diethylammonium chloride) was used as a model hydrophilic drug, while BODIPY 493/503 (4,4-difluoro-1,3,5,7-tetramethyl-4-bora-3a,4a-diaza-s-indacene-8-propionic acid) was utilized as a model hydrophobic drug. PCL was used as a hydrophobic scaffold and a 50:50 PCL-Gelatin blend as a hydrophilic scaffold. Dyes were infused into each scaffold in a variety of hydrophobicity match-mismatch conditions via supercritical and/or subcritical CO_2. Infusion by simple adsorption was used as a control. Release of dye over two weeks and the initial dye loading were measured to investigate and quantify the effects of drug-matrix interactions on controlled release. Visual observation of scaffolds before and after release was also used to draw qualitative conclusions. This study aims to improve understanding of polarity-based drug-drug and drug-matrix interactions within a dual infusion and release system. This understanding will enable the development of tightly controlled multi-drug release from CO_2 infused nanofiber scaffolds to better modulate complex regenerative medicine challenges such as chronic wound healing.

2 Materials and Methods

2.1 Polymer and dye solutions

Five wt.% polycaprolactone (PCL) (Sigma-Aldrich, St. Louis, MO; M_n 70-90 KDa) and 6.7 wt.% type A porcine gelatin (300 Bloom; Sigma-Aldrich, St. Louis, MO) solutions were produced by dissolution in 1,1,1,3,3,3-hexafluoro-2-propanol (HFP) (Oakwood Chemical, West Columbia, SC) at room temperature (~25^{o}C) for 24 hours with magnetic stirring. Initially separate solutions of PCL and gelatin were mixed in equal parts by volume and the combination stirred at room temperature (~25^{o}C) for 24 hours to create a hydrophilic blend. Pure PCL solution was used as a hydrophobic polymer. Solutions containing 0.1 mg/mL of Rhodamine B (Standard Fluka; Sigma-Aldrich, St. Louis, MO) and 0.1 mg/mL of BODIPY 493/503 (Life Technologies, Carlsbad, CA) were dissolved separately in 200 proof ethanol (Hedwin, Baltimore, MD). Dual dye solutions containing both 0.1 mg/mL Rhodamine B and 0.1 mg/mL BODIPY were also produced. Stirring at room temperature for 24 hours was necessary to dissolve BODIPY in ethanol solution. Both dye solutions were protected from photobleaching by wrapping the solution containers in aluminum foil and storing them in the dark when not in use.

2.2 Electrospinning

Solutions of PCL-gelatin blend and pure PCL were poured into 60 mL syringes, fitted with an 18 gage blunt tip needle, and mounted onto a syringe pump (kdScientific, Holliston, MA). Solutions were electrospun into 7.5 x 7.5 cm nanofiber sheets using a DC high voltage power supply (Glassman High Voltage, High Bridge, NJ) at 20 kV and a cathode to anode separation of 21 cm [33]. Flow rates and electrospinning time were

adjusted to ensure good fiber production, as shown in the SEM, and 10 mL of polymer solution was required to fabricate each scaffold. 'Core-shell' nanofibers were produced using a concentric needle attachment wherein PCL solution flowed through the center needle while PCL-gelatin solution flowed through a larger diameter needle surrounding it [34]. The previously listed electrospinning parameters were used for core-shell samples as well. The core to shell flow rate ratio was established at 1:4. 16 mm diameter disc samples were removed from as-produced nanofiber sheets using a metal arc punch (CS Osborn & Co, Harrison, NJ) and weighed. Only discs with weights between 20 and 30 mg were included in the study.

2.3 Dye Infusion

Disc samples were placed on a sheet of aluminum foil in a chemical fume hood. 500 μL of .1 mg/mL dye solution was adsorbed onto each scaffold in 100 μL increments; 10 minutes separated each application. Samples were allowed to dry at room temperature for 24 hours in the fume hood before infusion. The control scaffolds received no other infusion treatment but simple adsorption. Experimental scaffolds were lightly wrapped in aluminum foil and inserted into a stainless steel vessel for CO_2 infusion. CO_2 (Praxair, Columbus, OH) was compressed via a 1015 mL syringe pump (Teledyne ISCO, Lincoln, NE) to high pressures within the vessel. Scaffolds were exposed for 2 h to either subcritical CO_2 at 6.20 MPa at 25^{o}C or supercritical CO_2 at 8.27 MPa at 40^{o}C. After infusion, the vessel was depressurized slowly overnight. Temperature was maintained using a thermocouple system incorporated into the pressure vessel apparatus. Upon removal from the vessel, samples were rinsed within separate 15 mL vials with 70% ethanol in water for 30 minutes. Following rinsing, scaffolds were dried overnight in a

chemical fume hood and placed into fresh vials covered in aluminum foil. Dye loading was defined as the amount of dye remaining within the scaffold following the ethanol wash step.

2.4 Dye release

Scaffolds were soaked in 1 mL phosphate buffered saline (PBS) (AMRESCO, Solon, OH) plus 0.1 wt.% sodium azide (Sigma Aldrich, St. Louis, MO). At specified time points over the course of 2 weeks, the PBS was removed from each vial, stored in a 1.5 mL microcentrifuge tube (FisherBrand, Florence, KY), and replaced with 1 mL of fresh PBS. Aliquots of collected dye samples were placed into polystyrene 96 well plates (FisherBrand, Florence, KY) and analyzed with a fluorescence spectrophotometer (Spectra Max 190, Sunnyvale, CA) against a serial dilution of known dye concentrations.

2.5 Sample degradation

To quantify the dye retained by the sample after release was completed, each 16 mm disc was dissolved in 5 mL of HFP over 72 hours with 2 minutes of initial vortexing (VWR Vortex, VWR International, Radnor, PA). Degradation solutions were diluted by a factor of 5 in HFP. Aliquots of the diluted solutions were placed into polypropylene 96 well plates (FisherBrand, Florence, KY) and immediately analyzed with a fluorescence spectrophotometer against known dye concentrations. Loading values were acquired by summing the amount of dye released by degradation with the total amount of dye collected during the release process.

2.6 Scanning electron microscopy

Morphological changes before and after CO_2 exposure were analyzed using SEM. As spun samples, subcritical post-infusion samples, and supercritical post-infusion

samples were adhered to aluminum studs using carbon tape (Ted Pella, Reading, CA) and sputter-coated under argon gas with a 15 nm layer of Au-Pd (Pelco Model 3 sputter coater 91000, USA) at an emission current of 15 mA. Samples were examined by SEM (Quanta 300, Netherlands) allowing microstructural characterization at an accelerating voltage of 12 kV.

2.7 X-Ray diffraction

To measure changes in crystallinity following infusion, X-ray diffraction (XRD) (Ultima III, Rigaku Inc., Japan) utilizing a Cu X-ray source (40 kV) was conducted on samples before and after CO_2 infusion [35]. 22 mm diameter punches were removed from as spun PCL and core-shell nanofiber sheets and subjected to XRD analysis. The PCL punch was then subjected to subcritical infusion and the core-shell punch was subjected to supercritical infusion. Both samples were again analyzed using XRD over the range of 20-30^{o} 2θ.

2.8 Contact angle testing

Hydrophobicity of the different scaffolds was analyzed by contact angle measurement. Samples of PCL, PCL-gelatin, and core-shell nanofiber scaffolds were analyzed using a sessile drop method on an Easy Drop goniometer (Kruess, Hamburg, Germany). 400 μL of deionized water was placed onto the scaffold as a single drop and a screenshot taken after 3 seconds. Easy Drop software was utilized to calculate a contact angle based on the screenshot. Five measurements were taken for each type of scaffold and averaged.

2.9 Image analysis

Changes in the color of the punched samples over the course of release were visible to the naked eye. Representative images of PCL and PCL-gelatin infused with both dyes before and after the two week release process were taken using a bright field camera.

3 Results

3.1 Fiber morphology and microstructure

Electrospun nanofibers were imaged via SEM to observe their highly porous and fibrous microstructure. Figure 1 displays the SEM images of pre- (A-C) and post-CO_2 exposed (D-F) electrospun PCL, PCL-gelatin, and PCL 'core' PCL-gelatin 'shell' nanofibers. The unique microstructure of electrospun nanofiber provides a dense fibrous matrix closely resembling that of native tissue's extracellular matrix, especially the >80% porosity. Figure 1 (A,D) shows PCL fibers that are uniform, continuous, and free of beads or fiber-fiber bonds. Post-exposure to subcritical CO_2, only minor fiber-fiber bonding occurs without changes to the overall microstructure of the matrix or morphology of the fibers. PCL-gelatin nanofibers (Figure 1 (B,E)) pre- and post-subcritical CO_2 display no significant difference in microstructure or morphology as a result of exposure. Results from previous work have shown that supercritical conditions can result in significant alterations to PCL nanofiber microstructure and morphology resulting in a nearly film-like final state [24,35]. Interestingly, PCL 'core' PCL-gelatin 'shell' nanofibers display intact microstructure and porosity post-supercritical CO_2 exposure (Figure 1 (C,F)), suggesting that the PCL-gelatin shell has enough interaction with the pure PCL core to shield or protect it from CO_2-driven morphological alteration.

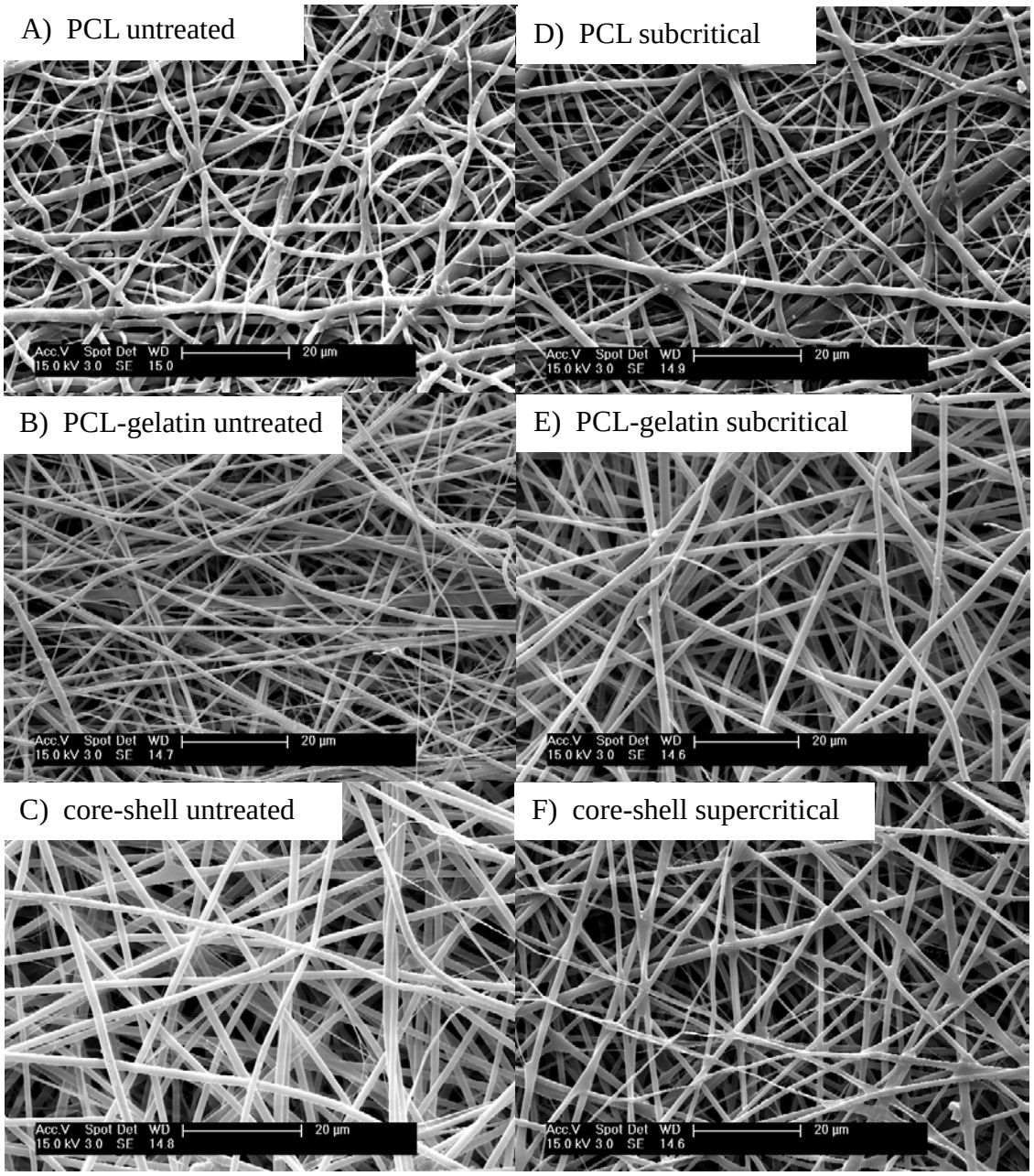

Figure 1: Scanning electron microscope images of untreated (A,B,C) and treated (D,E,F) PCL, PCL-gelatin, and PCL 'core' PCL-gelatin 'shell' nanofiber scaffolds, respectively. PCL and PCL-gelatin scaffolds were treated with subcritical (6.20 MPa, 25°C) CO_2 and core-shell scaffolds were treated with supercritical (8.27 MPa, 37°C) CO_2. All scaffolds retain clear nanofiber morphology after CO_2 exposure.

3.1.1 X-ray diffraction analysis

X-ray diffraction spectra (Figure 2) further imply that subcritical and supercritical CO_2 exposures do not cause significant alterations in the microstructure of PCL and core-shell nanofiber scaffolds, respectively. Interestingly, PCL and core-shell samples both show slight increases in intensity of the characteristic PCL crystal peaks (at 21.5 and 24° 2θ) following infusion.

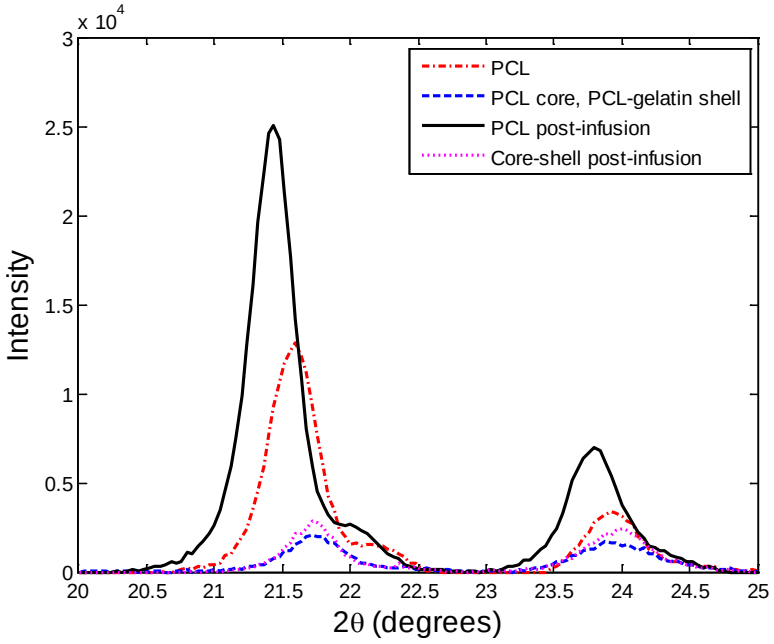

Figure 2: X-ray diffraction data from PCL and PCL 'core' PCL-gelatin 'shell' fibers pre- and post-infusion. Pure PCL fibers were infused subcritically at 6.20 MPa and 25°C while core-shell fibers were infused supercritically at 8.27 MPa and 40°C. An increase in intensity of characteristic PCL peaks at 21.5 and 24° 2θ post-infusion can be seen.

3.1.2 Contact angle testing

Contact angle experiments were used to validate the hypothesis that PCL constitutes a hydrophobic polymer and a 50:50 PCL-gelatin blend constitutes a

hydrophilic polymer. It was found that PCL had a wetting angle of 126.16 +/- 14.74 degrees. PCL-gelatin displayed a wetting angle of 0 degrees immediately after water droplets were placed onto it. By definition, PCL is considered hydrophobic and PCL-gelatin is considered hydrophilic.

3.2 Dye release behavior

Figure 3 displays an optical image of the electrospun nanofiber samples, initially saturated with equal concentrations of both BODIPY and Rhodamine B fluorescent dye, before and after release. Both the PCL and PCL-gelatin scaffolds (Figure 3 (A,B)) are dyed a similar red-purple color before release. Post-release images (Figure 3 (C,D)) show the color of the scaffolds with residual dye present after 334 hours of release.

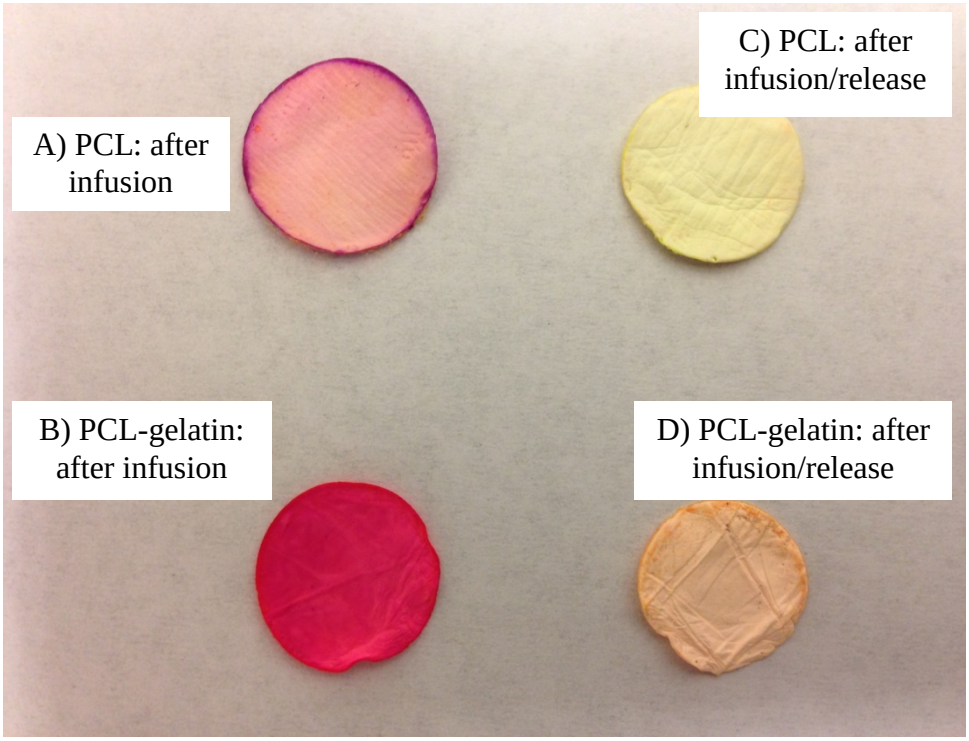

Figure 3: Visual appearance of PCL and PCL-gelatin after (A,B) subcritical CO_2 infusion of BODIPY+Rhodamine B at 6.20 MPa and 25°C and after (C,D) 334 hours of release in PBS. Scaffolds both appear a reddish-purple color before release. Post-release, PCL adopts the green color of BODIPY dye while PCL-gelatin is predominantly red in color, a characteristic of Rhodamine B dye.

PCL nanofiber scaffolds assume a yellow-green color post-release; PCL-gelatin appears have an orange-red tint post-release. This significant difference in color post-release confirms that BODIPY has a high affinity for PCL due to like hydrophobic interactions and that Rhodamine B has a high affinity to PCL-gelatin due to like hydrophilic interactions with the gelatin. Rhodamine in PCL and BODIPY in PCL-gelatin have been substantially released over the 334 hours due to unlike interactions.

Plots of release versus time confirm the optical observations (Figure 3), suggesting that hydrophobic-hydrophilic interactions can play a significant role in the release behaviors of the two different dyes. Figure 4 displays the percentage of total BODIPY (A) or Rhodamine B (B) released from PCL and from PCL-gelatin nanofiber scaffolds. BODIPY (Figure 4(A)) displays no significant difference in release percentage for adsorption-treated PCL or PCL-gelatin scaffolds, however significant differences in the release behavior and percentage of dye released are observed for nanofiber scaffolds treated with subcritical 6.20 MPa CO_2-assisted infusion. Subcritically-infused BODIPY PCL samples release 2.5% of their total loading, while PCL-gelatin releases 3.5%. The release behavior for subcritically infused BODIPY from PCL or PCL-gelatin scaffolds displayed an initial burst release (likely due to residual surface adsorbed dye), followed by linear release kinetics driven by diffusion. Rhodamine B release from PCL or PCL-gelatin scaffolds (Figure 4(B)) displays significant burst release kinetics for adsorbed PCL and PCL-gelatin for early time points. Subcritically infused PCL and PCL-gelatin showed similar burst release profiles until 72 hours, at which point release from PCL-gelatin continued while release from PCL stagnated. Adsorbed Rhodamine B exhibited

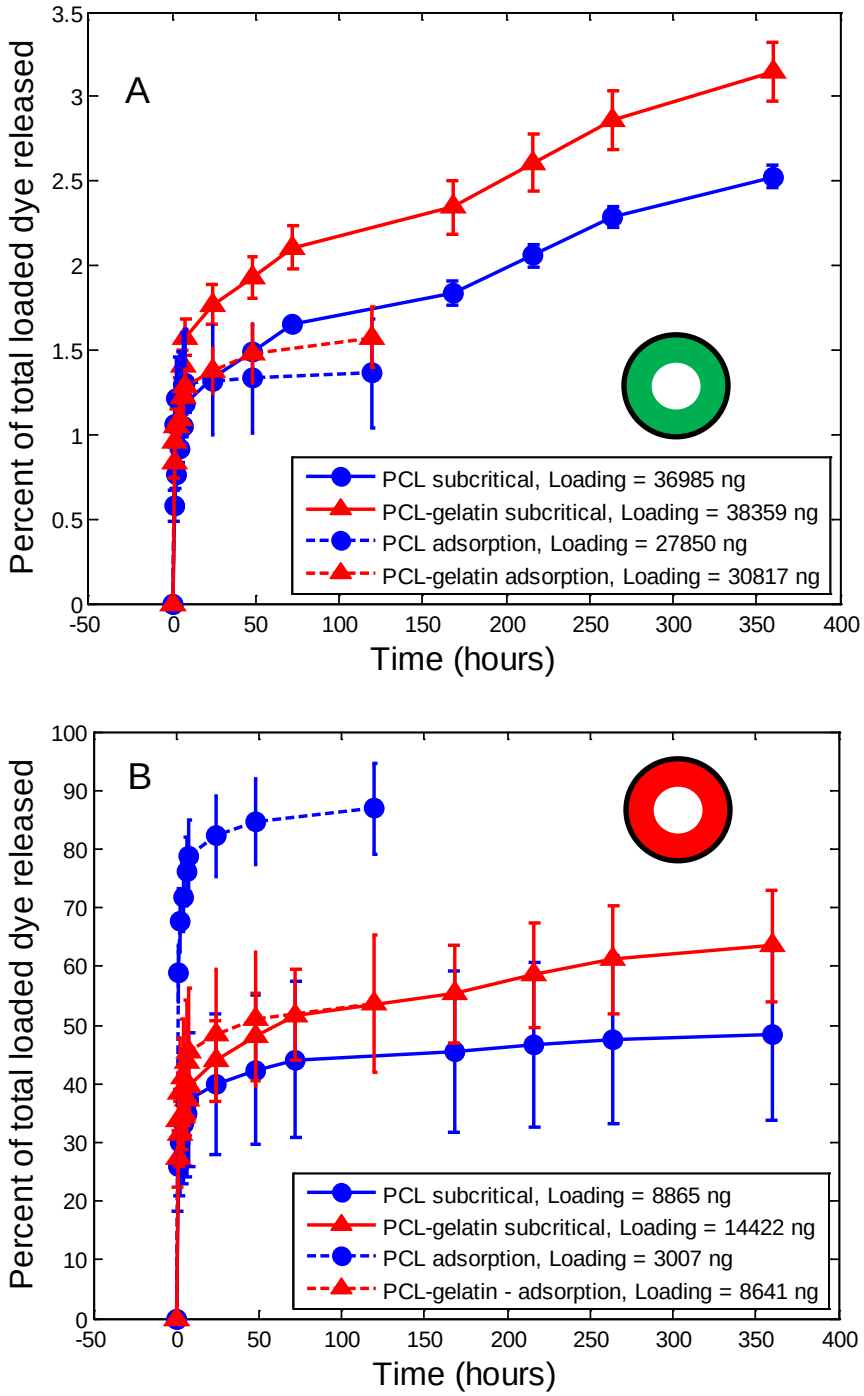

Figure 4: Release of A) BODIPY and B) Rhodamine B represented as a percent of initial scaffold loading following infusion of a single dye into PCL or PCL-gelatin. Total initial loading in ng is also given and is defined as the amount of dye in the scaffold after infusion and a 30 minute wash in 70% ethanol. Error bars represent one standard deviation in both directions. Colored circle in picture shows hypothesized dye localization in a fiber cross-section based on infusion condition.

nearly two-fold release from PCL scaffolds compared to PCL-gelatin, further illustrating favorable hydrophilic interactions between Rhodamine B and gelatin. No significant difference in the percentage released of total loaded Rhodamine B was observed between adsorption on PCL-gelatin and subcritical infusion on PCL or PCL-gelatin. However, in terms of amount of dye released, subcritically infused PCL-gelatin scaffolds released ~9000 ng of dye, statistically greater than all other conditions. Rhodamine B adsorption-treated PCL scaffolds released 84% of total loaded content within 24 hours, while PCL scaffolds treated with Rhodamine B by subcritical infusion released only 45% of their total content in this time.

Figure 5 displays the release of BODIPY (A) and Rhodamine B (B) from PCL and PCL-gelatin scaffolds treated with both dyes in equal concentrations via subcritical CO_2 or simple adsorption. BODIPY (Figure 5(A)) displays very little difference from single dye infusion (Figure 4(A)) in terms of percentage of dye released or release behavior. However, significant differences are noticed in Rhodamine B release when both dyes are present (Figure 5(B)). The release of subcritically infused Rhodamine B from PCL (unlike condition) increased by 20% over single dye-infused scaffolds, while release of subcritically infused Rhodamine B from PCL-gelatin (like condition) decreased by 40% compared to single dye conditions (Figure 4 (B)). This suggests that the goal of greater retention of 'like' dye and greater release of 'unlike' dye within a dual-dye system has been achieved. Furthermore, these results are evidence of competitive interaction between multiple dyes during the infusion and release process. No significant difference in the percentage of Rhodamine B released from adsorption-treated scaffolds was observed between single and dual dye infusion conditions (Figures 4(B) and 5(B)).

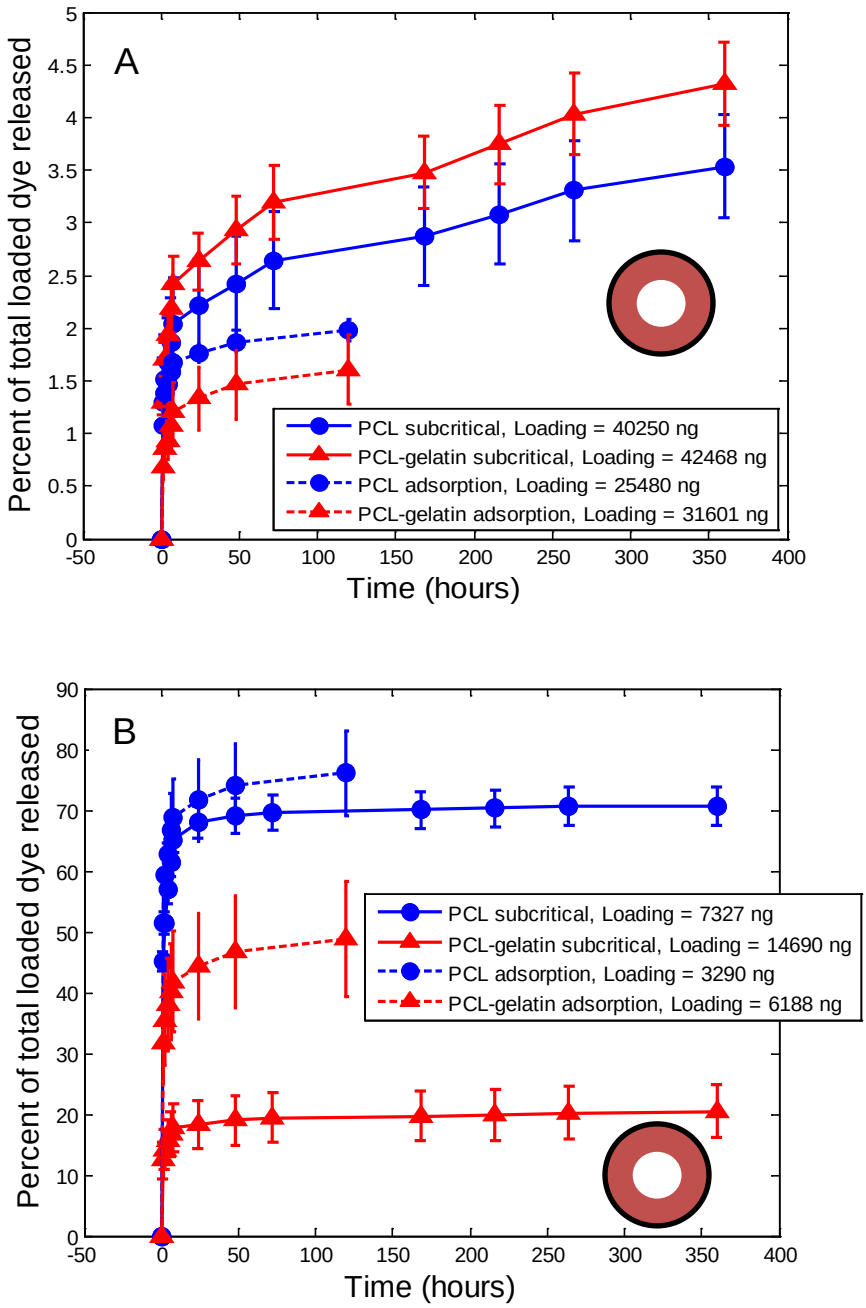

Figure 5: Release of A) BODIPY and B) Rhodamine B represented as a percent of initial scaffold loading following simultaneous infusion of both dyes into either PCL or PCL-gelatin. Initial loading in ng is also given. Release of Rhodamine B from PCL following subcritical CO_2 infusion is nearly twice that observed in Figure 4 (B), suggesting that addition of BODIPY to scaffold causes increased release of Rhodamine B. Error bars represent one standard deviation in both directions. Colored circle in picture shows hypothesized dye localization in a fiber cross-section based on infusion condition (purple = mixed).

Furthermore, for both BODIPY and Rhodamine B, core-shell scaffolds treated with both dyes (Figure 6(A,B)) using simple adsorption displayed release percentages statistically similar to PCL-gelatin scaffolds treated with adsorption of one or both dyes. These findings suggest that release of adsorbed drugs is statistically unaffected by infusion of additional dyes or use of composite scaffolds.

Figure 6(A) shows that, within PCL 'core' PCL-gelatin 'shell' scaffolds, supercritical infusion of BODIPY causes slower release compared to BODIPY infused under subcritical conditions. This trend is opposite that for Rhodamine B infused scaffolds, displaying increased release percentages for supercritically infused scaffolds as compared to subcritically infused nanofiber scaffolds. These observations suggest that supercritically infused BODIPY and subcritically infused Rhodamine B are experiencing favorable interactions with the scaffold, while subcritically infused BODIPY and supercritically infused Rhodamine B are experiencing unfavorable interactions. Therefore, high penetration supercritical infusion likely infuses dye into the hydrophobic core while lower penetration subcritical infusion likely infuses dye into the hydrophilic shell.

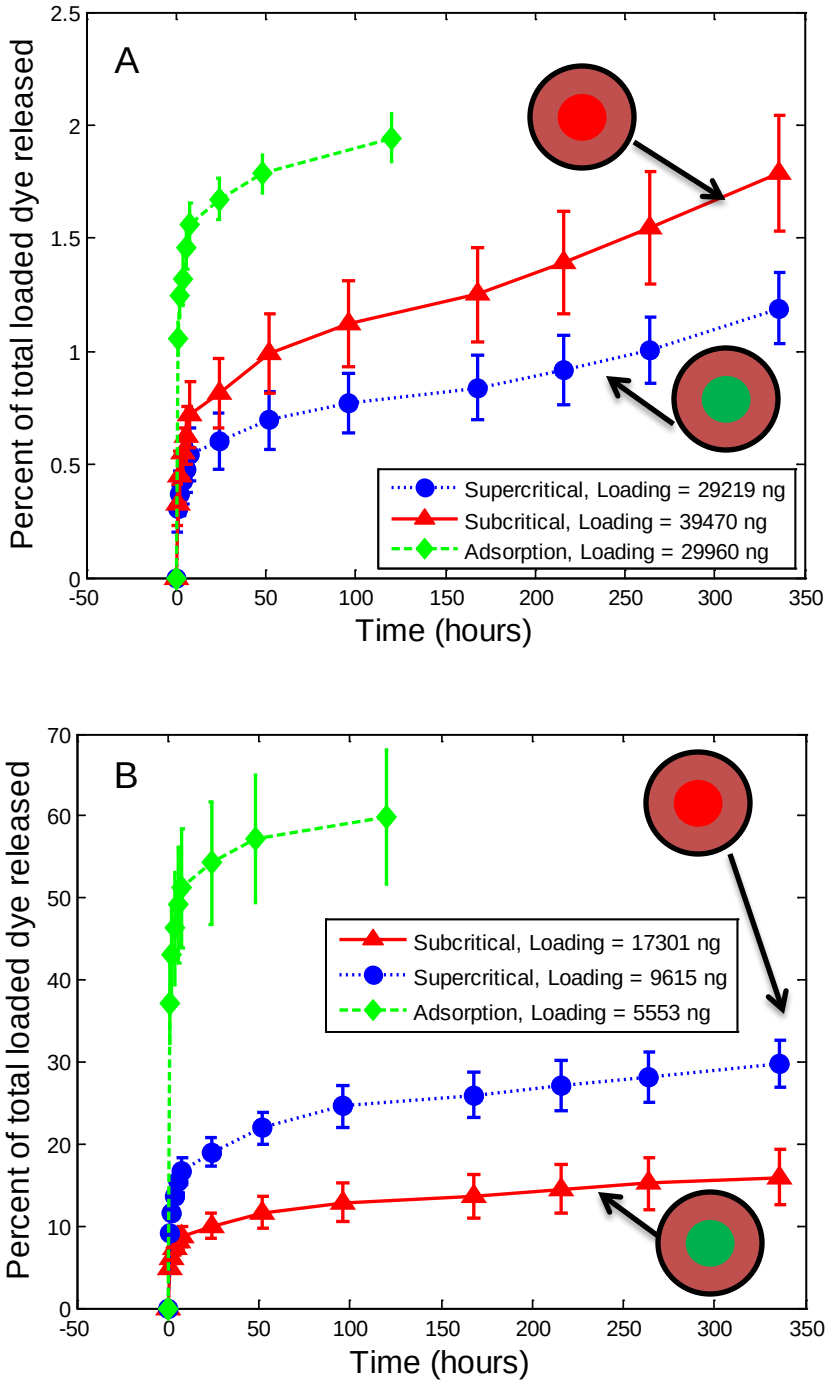

Figure 6: Release of A) BODIPY and B) Rhodamine B represented as a percent of initial scaffold loading following infusion into PCL 'core' PCL-gelatin 'shell' nanofibers using either subcritical infusion, supercritical infusion, or simple adsorption conditions. Initial loading in ng is also given. The percentage release following adsorption is very similar to that of Figure 5 as anticipated given that the exterior surface of the nanofiber is identical. Error bars represent one standard deviation in both directions. Colored circle in picture shows hypothesized dye localization in a fiber cross-section based on infusion condition.

3.3. Dye infusion and loading analysis

To further corroborate evidence of the effects that hydrophobic-hydrophilic interactions have on drugs infused into nanofiber scaffolds via CO_2, differential loading of dyes was also quantified. Figure 7(A) displays the total loaded BODIPY content in PCL or PCL-gelatin nanofiber scaffolds treated using either subcritical CO_2 or simple adsorption. Subcritical CO_2 infusion of BODIPY into PCL or PCL-gelatin scaffolds displayed significantly greater loading than adsorption, amounting to approximately a 30% increase. No significant differences in loading were observed between PCL and PCL-gelatin scaffolds (Figure 7(A)). Similar trends were observed for BODIPY loading when both dyes were infused into PCL or PCL-gelatin scaffolds, resulting in a net 45% increase over simple adsorption. No significant differences were observed in the loading of BODIPY between single and dual dye adsorption. Figure 7(B) shows that supercritical infusion resulted in no significant differences in loading compared to adsorption. Subcritical infusion of BODIPY resulted in a 33% increase in loading compared to adsorption. Loading of Rhodamine B into PCL or PCL-gelatin scaffolds (Figure 8(A)) and into core-shell samples (Figure 8(B)) further showed that significant improvements in loading were achieved when CO_2 infusion was utilized over adsorption. Subcritical CO_2 infusion resulted in nearly 2-fold increases in Rhodamine B loading compared to adsorption on hydrophilic PCL-gelatin. Nearly a 3-fold increase in loading over adsorption was achieved for Rhodamine B infused into hydrophobic PCL nanofibers by subcritical CO_2. Similar trends were observed for core-shell scaffolds (Figure 8(B)), showing a significant increase in loading for supercritical and subcritical infusion of Rhodamine B over simple adsorption.

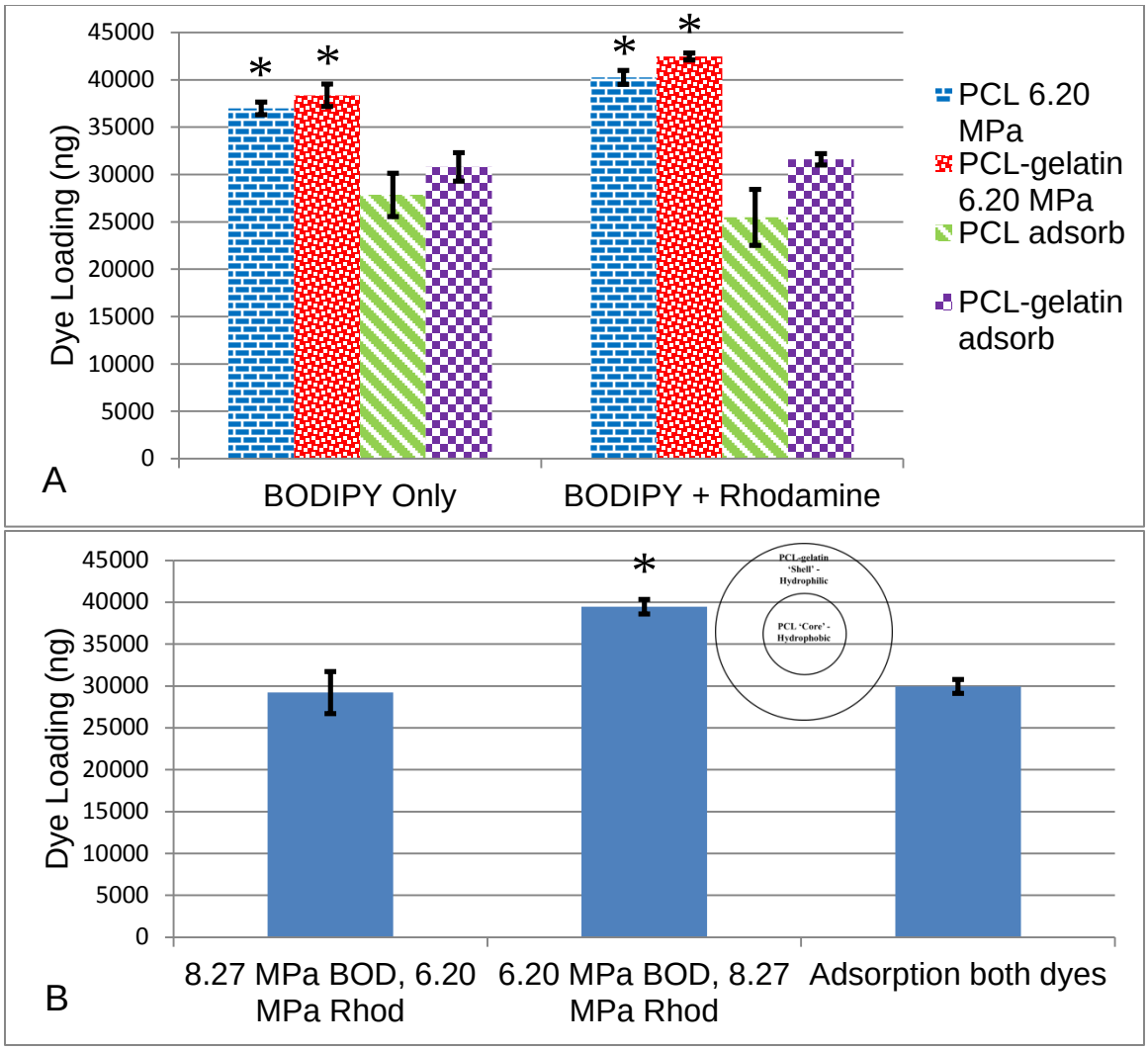

Figure 7: A) Absolute BODIPY loading into either PCL or PCL-gelatin. Subcritical CO_2 exposure increases dye loading over simple adsorption by ~50% for PCL and ~30% for PCL-gelatin. B) Absolute BODIPY loading into PCL 'core' PCL-gelatin 'shell' nanofibers under subcritical (6.20 MPa, 25°C) and supercritical (8.27 MPa, 40°C) CO_2 conditions versus simple adsorption at 25°C. The schematic in the figure displays the cross-section of a core-shell fiber. Supercritical CO_2 exposure does not result in any statistical difference of BODIPY loading into these scaffolds compared to adsorption. *Significantly different from adsorption condition ($p < .05$).

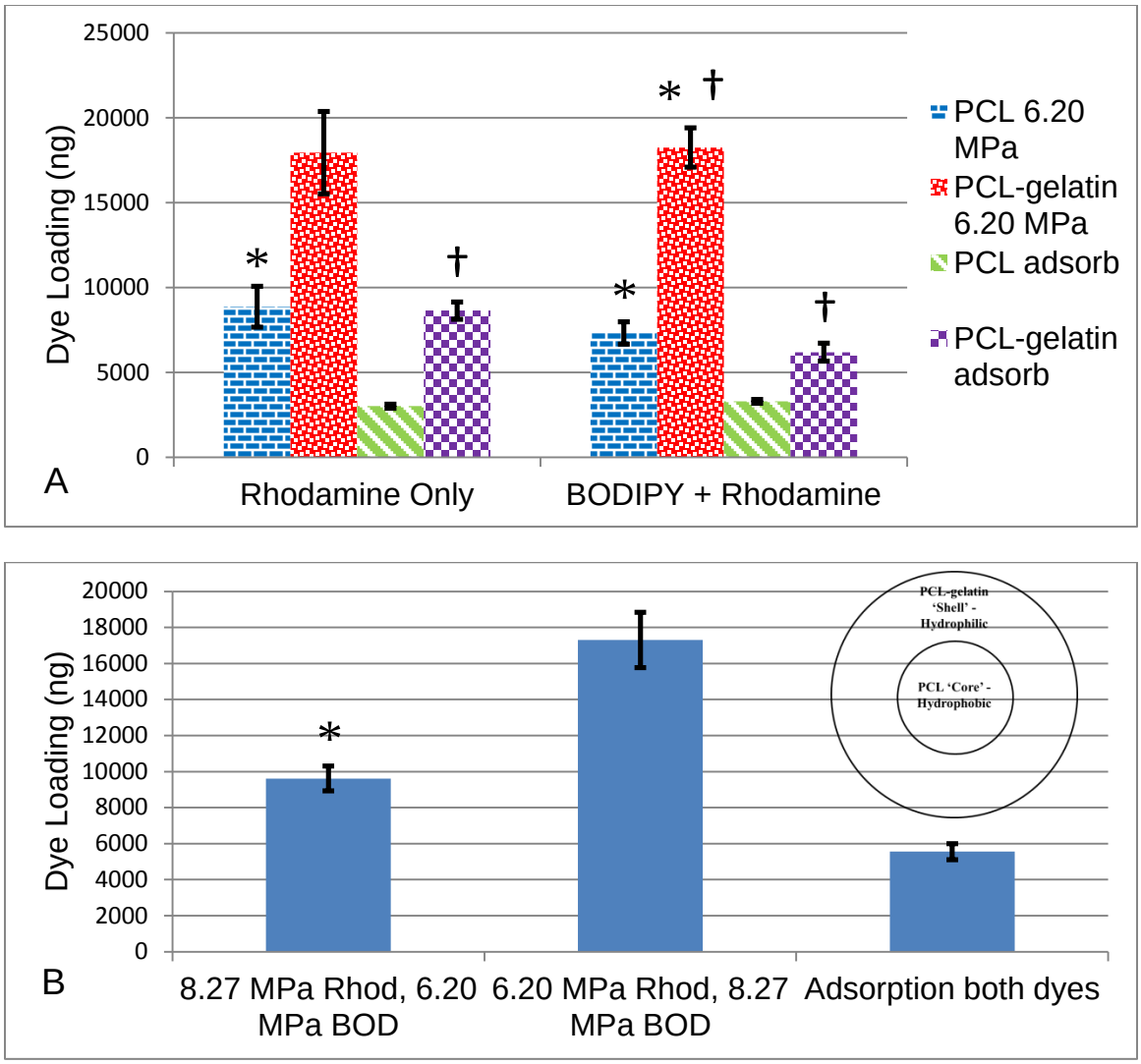

Figure 8: A) Absolute Rhodamine B loading into either PCL or PCL-gelatin under subcritical CO_2 conditions versus simple adsorption at 25°C. Subcritical CO_2 exposure increases dye loading over simple adsorption by ~300% for PCL and ~200% for PCL-gelatin. B) Absolute Rhodamine B loading into PCL 'core' PCL-gelatin 'shell' nanofibers under subcritical (6.2MPa, 25°C) and supercritical (8.27 MPa, 40°C) CO_2 conditions versus simple adsorption at 25°C. Core-shell schematic is shown above the adsorption bar. Supercritical CO_2 exposure increases Rhodamine B loading by ~100% over simple adsorption and subcritical CO_2 exposure increases Rhodamine B loading by ~200% over adsorption. *Significantly different from adsorption condition ($p < .05$) †Significantly different from PCL under same condition ($p < .05$)

4. Discussion

4.1 Effects of CO_2 infusion on nanofiber morphology and microstructure

The capability of pressurized CO_2 to plasticize polymers is well understood and frequently utilized as a processing technique in industry. Pressurized CO_2 has recently gained interest within the research realm as a benign, green, and inexpensive technique to embed small molecules into polymer matrices. As such, CO_2 is an attractive vehicle for biomolecule infusion directed towards tissue engineering efforts. Previous studies in our group [35] have shown varying biomolecule infusion and release behavior with alterations in pressure and phase of CO_2. Dense subcritical CO_2 provides moderate plasticization, leading to some impregnation of biomolecules beneath the surface of a polymer matrix, enabling prolonged release. Supercritical CO_2 fully plasticizes the polymer material, embedding molecules deep within the matrix and enabling steady release. Based on these properties of the different phases, our group has hypothesized that within core-shell scaffolds, subcritical CO_2 infuses drugs into the shell region of the fiber, while supercritical CO_2 can infuse drugs all the way into the core. Both phases of CO_2 melt most of the crystalline regions of polymers before swelling can occur. However, the swelling process increases free volume and chain mobility, allowing crystalline microstructure to reform and grow extensively during slow depressurization [36] . This process is evident in XRD spectra (Figure 2), in which the crystalline peaks characteristic of PCL are more intense after infusion. While microstructural changes during the infusion process are generally reversible, supercritical CO_2 is so effective in swelling certain polymers, such as PCL, that it destroys the nanoscale scaffold morphology, potentially eliminating useful properties that depend on scaffold

microstructure [24, 37-41]. To prevent this phenomenon from damaging electrospun nanofibers and to preserve their valuable microstructure for tissue engineering applications, PCL is blended in equal parts with porcine gelatin. Gelatin undergoes dehydration upon exposure to supercritical CO_2, causing it to compress and prevent excessive PCL chain motion that would ordinarily denature nanofiber morphology [35]. SEM imaging in Figure 1 shows evidence of nanofiber morphology both before and after supercritical CO_2 exposure. Interestingly, the core-shell nanofibers are unaffected by supercritical CO_2 exposure even though the core is pure PCL. The PCL-gelatin shell could conceivably protect the core by physically restraining it as it liquefies [42].

4.2 Hydrophobic-hydrophilic interactions and CO_2-infused dye loading

Interactions between drug and matrix play an important role in drug release kinetics, particularly in diffusion-based systems. While PCL and blended PCL-gelatin are both biodegradable polymers, neither loses an appreciable amount of mass over the release period and therefore release from these scaffolds is governed solely by diffusion. Hydrophobic-hydrophilic interactions are an appealing target for investigation as they can be easily manipulated with drug selection, scaffold plasma treatment, and polymer blending [43]. Hydrophobicity differences between drug and scaffold should exert a profound but predictable effect on drug loading. We observed that dyes infused into scaffolds with moieties of the same polarity experienced high loading, while the hydrophilic dye Rhodamine B exhibited reduced loading when infused into hydrophobic PCL. Based on the high loading shown in Figure 7, it would appear that BODIPY still interacts strongly with a PCL-gelatin blend based on a 50% composition of hydrophobic PCL chains. Loading of BODIPY was significantly greater than loading of Rhodamine B

under all conditions. This is reasonable as the wash solution used was 70% ethanol in water, a very hydrophilic mixture. This solvent was likely able to remove surface-bound Rhodamine B from the scaffold more effectively than BODIPY regardless of infusion condition.

Almost twice as much Rhodamine B was loaded into scaffolds by infusion compared to adsorption. BODIPY was loaded on average 45% more effectively by subcritical infusion versus adsorption. CO_2 infusion accomplishes this by plasticizing PCL, enabling impregnation of dye deeper into the polymer bulk. CO_2 infusion is therefore an effective tool to artificially introduce and control drug-matrix interactions within nanofiber scaffolds. Surprisingly, loading was found to be higher for dyes when subcritically infused into core-shell scaffolds versus supercritically infused. In its supercritical fluid phase, CO_2 may be dissolving and leaching dye from the scaffolds during infusion. This is plausible given the results of a study by Zhao et al., which revealed increasing solubility of Rhodamine B with increasing pressure of CO_2, as well as an intrinsically high solubility of nonpolar dyes like BODIPY in supercritical CO_2 [44].

4.3 Hydrophobic-hydrophilic interactions and CO_2 Infused dye release

Similarly, hydrophobic-hydrophilic interactions between drug and scaffold affect release properties. Previous literature suggests that stronger drug-matrix interactions allows for slower, more linear release while negative or lack of interaction promotes burst or rapid release [45]. BODIPY exhibited slow and limited release from all scaffolds, due to both a strong interaction with hydrophobic PCL domains found in all scaffolds as well as poor interactions with PBS as a release solvent. Rhodamine B, on the other hand,

showed much faster release from hydrophobic PCL than hydrophilic PCL-gelatin, as evidenced by Figures 4(B), and 5(B). Furthermore, comparison of Figures 4 and 5 shows that when two drugs were present, the drug with polarity similar to a given scaffold released more slowly and the drug with unlike polarity to a scaffold released more quickly. The release effect of interactions is further illustrated in Figure 3, where scaffolds initially infused with both dyes visibly retain only the 'like' dye after a 14 day infusion period.

Infusion by CO_2 embeds the drugs within the polymer bulk which necessitates interactions with the polymer chains before release can occur. While PCL displayed a burst release of adsorbed Rhodamine B within 48 hours, this was reduced by nearly half when Rhodamine B was infused into PCL via subcritical CO_2. Interactions enacted by CO_2 impregnation appear to have a more pronounced effect when infusing a hydrophilic dye into a hydrophobic scaffold or vice-versa [46]. A similar tactic for linearizing release was employed in a study by Yoon and Kim, wherein Rhodamine-releasing polyethylene oxide (PEO) nanofibers were embedded in mats of PCL nanofibers of varying thickness. In concordance with the results of our study, Yoon et al. found that thicker layers of hydrophobic PCL reduced burst release and encourage slower, more linear release [32].

4.3.1 Interactions and CO_2 infusion in core-shell scaffolds for multi-drug release

Exposure to either sub- or supercritical CO_2 plasticizes PCL and PCL-gelatin enough to allow infusion of model drug compounds either singly or in concert. Even at subcritical pressures, polymer free volume is enhanced sufficiently to enable the greater mobility needed to allow for interdiffusion of these model drug compounds among the polymer chains and enhance the total loading above that created by either simple

adsorption or chemical attachment on high surface area nanofiber substrates. The greater intermolecular interactions of the hydrophobic PCL with BODIPY results in preferred partitioning of that compound within the PCL core. Similarly, the greater intermolecular interactions of the hydrophilic gelatin with Rhodamine B results in preferred partitioning of that compound within the PCL-gelatin shell. Using different phases of CO_2 can further modulate drug localization in core-shell nanofibers, providing facile control of loading and release behavior. Subcritical CO_2 infusion induces preferred partitioning into the superficial shell while supercritical CO_2 induces preferred partitioning into the core.

Figure 6 displays very slow, linear release when BODIPY is infused into a PCL core with supercritical CO_2 and when Rhodamine B is infused into a PCL-Gelatin shell using subcritical CO_2. Infusing BODIPY into the shell or Rhodamine B into the core leads to faster release while simple adsorption leads to a rapid initial burst of drug release. These observations are consistent with the interaction-release relationship anticipated for these drug-matrix combinations and validate that CO_2 infusion and drug-matrix interactions can be effectively utilized to biofunctionalize electrospun nanofiber scaffolds and tailor the release profile of multiple biomolecules within such scaffolds. Past experiments with CO_2 infusion have shown that supercritically infused dyes or drugs tend to display slower, steadier release than subcritically infused dyes. This behavior was expected for both dyes when infused into core-shell fibers. Interestingly, Figure 6 reveals that Rhodamine B released slower and steadier when subcritically infused into the shell compared to supercritically infused into the core. These data support the hypothesis that

in CO_2 infused nanofiber systems, interactions have a greater effect on release properties than phase of CO_2.

4.4 Applications in Tissue Engineering

Wound management requires an ECM-resemblant, fluid absorbing, gas permeable, non-adhesive dressing, making electrospun nanofibers an excellent fit for the demands of the condition [47]. Chronic wounds, however, require more than just a suitable scaffold. Significant infection, underlying neuropathy and/or vascular degeneration must be addressed before substantial regeneration can occur. This has been accomplished with some level of success by application of growth factors, such as PDGF, bFGF, and VEGF to the wound area [48]. However, topical application of drugs alone fails to realize their maximum potential [29] and high doses of these growth factors are known to increase the patient's risk for cancer. Studies have also shown that unaddressed infection in chronic wounds greatly inhibits the healing process [48]. A CO_2 infused nanofiber patch with controlled bimodal release capabilities provides a solution to this problem. To immediately address infection, a small molecule antibacterial drug, like mupirocin, would be rapidly released from the scaffold. Underlying pathology would be addressed by steady, long term release of a growth factor, which would peak in its cumulative release towards the end of the healing process. Based on the results of this study, this could be accomplished using hydrophilic polymer nanofibers, with hydrophobic mupirocin infused subcritically and hydrophilic PDGF infused supercritically.

5. Conclusions

Electrospun nanofibers are promising materials for tissue engineering applications, especially chronic wounds. CO_2 infusion technology can further augment nanofiber biomaterials by incorporating bioactivity through growth factors and other biomolecules. CO_2 infusion holds advantages over other methods for drug infusion in that it is an inexpensive, green, and bioactivity-preserving vector for impregnation. This study used dyes to provide a better understanding of the effects of hydrophobic-hydrophilic interactions within CO_2 infused nanofiber systems. This type of drug-matrix interaction should be strong in order to elicit long-term, linear release but weak if the goal is to elicit rapid burst release of drug. CO_2 infusion provides an approach to engineer such strong interactions and achieve desirable release profiles by embedding different drugs within the nanofiber scaffold. In particular, biphasic core-shell nanofiber scaffolds can achieve an even greater level control over release using different phases of CO_2 to partition drugs within composite scaffolds. Future work will capitalize on this high level of control to build a core-shell nanofiber scaffold capable of bimodal release of two biomolecules relevant to chronic wound healing.

5.1 Future Work

Ultimately, our group intends to utilize the preferred partitioning effects of the different phases of CO_2 in core-shell nanofibers to design drug-matrix interactions for a target release profile. Bimodal release is of particular interest to us for applications in tissue engineering. From a nanofiber patch, a small molecule drug could be released immediately while a larger, protein based therapeutic would be released steadily over time, peaking in cumulative release towards the end of treatment. Previous studies within the group have shown a significant, yet uncharacterized, effect of infused particle size on

release properties from CO_2 infused nanofiber scaffolds. Before clinically focused studies with protein based drugs can be conducted, this effect must be better understood. Current work is focused on a pilot study on this effect. In a factorial experimental design, Rhodamine B (2 nm hydrodynamic diameter), Green Q-Dots (4 nm hydrodynamic diameter), and FITC-labeled bovine serum albumin (7 nm hydrodynamic diameter), will be subcritically infused into PCL nanofibers with or without air plasma treatment (to account for surface hydrophilicity). Each size-plasma treatment condition will be run 4 times for a total of 24 runs. We expect to observe either a linear relationship between particle size and release properties, or possibly a size cutoff at which subcritical CO_2 infusion does not affect release properties. Data acquired from this study will be useful in development of the CO_2 infused nanofiber system towards controlled release of clinically relevant compounds.

References

[1] T. Gilchrist, A.M. Martin, Wound treatment with Sorbsan — an alginate fibre dressing, Biomaterials. 4 (1983) 317-320.

[2] R. FRASER, T. GILCHRIST, Sorbsan Calcium Alginate Fiber Dressings in Footcare, Biomaterials. 4 (1983) 222-224.

[3] R. OLIVER, H. BARKER, A. COOKE, R. GRANT, Dermal Collagen Implants, Biomaterials. 3 (1982) 38-40.

[4] F. Caiado, T. Carvalho, F. Silva, C. Castro, N. Clode, J.F. Dye, S. Dias, The role of fibrin E on the modulation of endothelial progenitors adhesion, differentiation and angiogenic growth factor production and the promotion of wound healing, Biomaterials. 32 (2011) 7096-7105.

[5] F. Mi, S. Shyu, Y. Wu, S. Lee, J. Shyong, R. Huang, Fabrication and characterization of a sponge-like asymmetric chitosan membrane as a wound dressing, Biomaterials. 22 (2001) 165-173.

[6] P.T. Sudheesh Kumar, N.M. Raj, G. Praveen, K.P. Chennazhi, S.V. Nair, R. Jayakumar, In vitro and in vivo evaluation of microporous chitosan hydrogel/nanofibrin composite bandage for skin tissue regeneration. Tissue engineering.Part A. 19 (2013) 380-392.

[7] G. BIAGINI, A. BERTANI, R. MUZZARELLI, A. DAMADEI, G. DIBENEDETTO, A. BELLIGOLLI, G. RICCOTTI, C. ZUCCHINI, C. RIZZOLI, Wound Management with N-Carboxybutyl Chitosan, Biomaterials. 12 (1991) 281-286.

[8] E. Matouskova, L. Broz, V. Stolbova, L. Klein, R. Konigova, P. Vesely, Human allogeneic keratinocytes cultured on acellular xenodermis: The use in healing of burns and other skin defects, Biomed. Mater. Eng. 16 (2006) S63-S71.

[9] J.W. Drexler, H.M. Powell, Regulation of electrospun scaffold stiffness via coaxial core diameter, Acta Biomater. 7 (2011) 1133-1139.

[10] N. Zaari, P. Rajagopalan, S. Kim, A. Engler, J. Wong, Photopolymerization in microfluidic gradient generators: Microscale control of substrate compliance to manipulate cell response, Adv Mater. 16 (2004) 2133-+.

[11] R. MILLER, J. BRADY, D. CUTRIGHT, Degradation Rates of Oral Resorbable Implants (Polylactates and Polyglycolates) - Rate Modification with Changes in Pla-Pga Copolymer Ratios, J. Biomed. Mater. Res. 11 (1977) 711-719.

[12] H. Pan, H. Jiang, W. Chen, Interaction of dermal fibroblasts with electrospun composite polymer scaffolds prepared from dextran and poly lactide-co-glycolide, Biomaterials. 27 (2006) 3209-3220.

[13] V.J. Reddy, S. Radhakrishnan, R. Ravichandran, S. Mukherjee, R. Balamurugan, S. Sundarrajan, S. Ramakrishna, Nanofibrous structured biomimetic strategies for skin tissue regeneration, Wound Repair Regen. 21 (2013) 1-16.

[14] M. Khil, D. Cha, H. Kim, I. Kim, N. Bhattarai, Electrospun nanofibrous polyurethane membrane as wound dressing, J. Biomed. Mater. Res. Part B. 67B (2003) 675-679.

[15] V. Leung, F. Ko, Biomedical applications of nanofibers, Polym. Adv. Technol. 22 (2011) 350-365.

[16] S.A. Sell, M.J. McClure, K. Garg, P.S. Wolfe, G.L. Bowlin, Electrospinning of collagen/biopolymers for regenerative medicine and cardiovascular tissue engineering, Adv. Drug Deliv. Rev. 61 (2009) 1007-1019.

[17] K. Rho, L. Jeong, G. Lee, B. Seo, Y. Park, S. Hong, S. Roh, J. Cho, W. Park, B. Min, Electrospinning of collagen nanofibers: Effects on the behavior of normal human keratinocytes and early-stage wound healing, Biomaterials. 27 (2006) 1452-1461.

[18] Y.B. Truong, V. Glattauer, K.L. Briggs, S. Zappe, J.A.M. Ramshaw, Collagen-based layer-by-layer coating on electrospun polymer scaffolds, Biomaterials. 33 (2012) 9198-9204.

[19] Y.M. Shin, H. Shin, Y.M. Lim, Surface Modification of Electrospun Poly(L-lactide-co-epsilon-caprolactone) Fibrous Meshes with a RGD Peptide for the Control of Adhesion, Proliferation and Differentiation of the Preosteoblastic Cells, Macromol. Res. 18 (2010) 472-481.

[20] W. Ji, F. Yang, J.J.J.P. van den Beucken, Z. Bian, M. Fan, Z. Chen, J.A. Jansen, Fibrous scaffolds loaded with protein prepared by blend or coaxial electrospinning, Acta Biomater. 6 (2010) 4199-4207.

[21] M.V. Natu, H.C. de Sousa, M.H. Gil, Electrospun Drug-Eluting Fibers for Biomedical Applications, Stud. Mechanobiol. Tissue Eng. Biomater. 8 (2011) 57-85.

[22] F. Chen, M. Zhang, Z. Wu, Toward delivery of multiple growth factors in tissue engineering, Biomaterials. 31 (2010) 6279-6308.

[23] P.A. Madurantakam, I.A. Rodriguez, M.J. Beckman, D.G. Simpson, G.L. Bowlin, Evaluation of biological activity of bone morphogenetic proteins on exposure to commonly used electrospinning solvents, J. Bioact. Compatible Polym. 26 (2011) 578-589.

[24] O. Ayodeji, E. Graham, D. Kniss, J. Lannutti, D. Tomasko, Carbon dioxide impregnation of electrospun polycaprolactone fibers, J. Supercrit. Fluids. 41 (2007) 173-178.

[25] T. Sproule, J. Lee, H. Li, J. Lannutti, D. Tomasko, Bioactive polymer surfaces via supercritical fluids, J. Supercrit. Fluids. 28 (2004) 241-248.

[26] P.J. Ginty, J.J.A. Barry, L.J. White, S.M. Howdle, K.M. Shakesheff, Controlling protein release from scaffolds using polymer blends and composites, European Journal of Pharmaceutics and Biopharmaceutics. 68 (2008) 82-89.

[27] C.K. Sen, G.M. Gordillo, S. Roy, R. Kirsner, L. Lambert, T.K. Hunt, F. Gottrup, G.C. Gurtner, M.T. Longaker, Human skin wounds: A major and snowballing threat to public health and the economy, Wound Repair Regen. 17 (2009) 763-771.

[28] P. Losi, E. Briganti, C. Errico, A. Lisella, E. Sanguinetti, F. Chiellini, G. Soldani, Fibrin-based scaffold incorporating VEGF- and bFGF-loaded nanoparticles stimulates wound healing in diabetic mice, Acta Biomater. 9 (2013) 7814-7821.

[29] R.A. Thakur, C.A. Florek, J. Kohn, B.B. Michniak, Electrospun nanofibrous polymeric scaffold with targeted drug release profiles for potential application as wound dressing, Int. J. Pharm. 364 (2008) 87-93.

[30] B. Jiang, G. Zhang, E.M. Brey, Dual delivery of chlorhexidine and platelet-derived growth factor-BB for enhanced wound healing and infection control, Acta Biomater. 9 (2013) 4976-4984.

[31] Z. Xie, C.B. Paras, H. Weng, P. Punnakitikashem, L. Su, K. Vu, L. Tang, J. Yang, K.T. Nguyen, Dual growth factor releasing multi-functional nanofibers for wound healing. Acta biomaterialia. 9 (2013) 9351-9359.

[32] H. Yoon, G. Kim, A Three-Dimensional Polycaprolactone Scaffold Combined with a Drug Delivery System Consisting of Electrospun Nanofibers, J. Pharm. Sci. 100 (2011) 424-430.

[33] J. Gaumer, A. Prasad, D. Lee, J. Lannutti, Structure-function relationships and source-to-ground distance in electrospun polycaprolactone, Acta Biomater. 5 (2009) 1552-1561.

[34] J. Nam, J. Johnson, J.J. Lannutti, S. Agarwal, Modulation of embryonic mesenchymal progenitor cell differentiation via control over pure mechanical modulus in electrospun nanofibers, Acta Biomater. 7 (2011) 1516-1524.

[35] M.T. Nelson, H.R. Munj, D.L. Tomasko, J.J. Lannutti, Carbon dioxide infusion of composite electrospun fibers for tissue engineering, J. Supercrit. Fluids. 70 (2012) 90-99.

[36] G. Verreck, A. Decorte, H. Li, D. Tomasko, A. Arien, J. Peeters, P. Rombaut, G. Van den Mooter, M.E. Brewster, The effect of pressurized carbon dioxide as a plasticizer and foaming agent on the hot melt extrusion process and extrudate properties of pharmaceutical polymers, J. Supercrit. Fluids. 38 (2006) 383-391.

[37] D. Gallego-Perez, N. Higuita-Castro, S. Sharma, R.K. Reen, A.F. Palmer, K.J. Gooch, L.J. Lee, J.J. Lannutti, D.J. Hansford, High throughput assembly of spatially controlled 3D cell clusters on a micro/nanoplatform, Lab Chip. 10 (2010) 775-782.

[38] D.E. Heath, J.J. Lannutti, S.L. Cooper, Electrospun scaffold topography affects endothelial cell proliferation, metabolic activity, and morphology, J. Biomed. Mater. Res. Part A. 94A (2010) 1195-1204.

[39] J. Johnson, M.O. Nowicki, C.H. Lee, E.A. Chiocca, M.S. Viapiano, S.E. Lawler, J.J. Lannutti, Quantitative Analysis of Complex Glioma Cell Migration on Electrospun Polycaprolactone Using Time-Lapse Microscopy, Tissue Eng. Part C-Methods. 15 (2009) 531-540.

[40] S. Drilling, J. Gaumer, J. Lannutti, Fabrication of burst pressure competent vascular grafts via electrospinning: Effects of microstructure, J. Biomed. Mater. Res. Part A. 88A (2009) 923-934.

[41] H. Powell, D. Kniss, J. Lannutti, Nanotopographic control of cytoskeletal organization, Langmuir. 22 (2006) 5087-5094.

[42] R. Xue, P. Behera, J. Xu, M.S. Viapiano, J.J. Lannutti, Polydimethylsiloxane coreâ€“polycaprolactone shell nanofibers as biocompatible, real-time oxygen sensors, Sensors Actuators B: Chem. 192 (2014) 697-707.

[43] K. Kull, M. Steen, E. Fisher, Surface modification with nitrogen-containing plasmas to produce hydrophilic, low-fouling membranes, J. Membr. Sci. 246 (2005) 203-215.

[44] C. Zhao, J. Wang, I. Tabata, T. Hori, Solubility of Rhodamine B in Supercritical Carbon Dioxide Fluids with or without Cosolvent, Advanced Textile Materials, Pts 1-3. 332-334 (2011) 146-151.

[45] J. Zeng, L. Yang, Q. Liang, X. Zhang, H. Guan, X. Xu, X. Chen, X. Jing, Influence of the drug compatibility with polymer solution on the release kinetics of electrospun fiber formulation, J. Controlled Release. 105 (2005) 43-51.

[46] Wang Li-hong, Che Xin, Xu Hui, Zhou Li-li, Han Jing, Zou Mei-juan, Liu Jie, Liu Yi, Liu Jin-wen, Zhang Wei, Cheng Gang, A novel strategy to design sustained-release poorly water-soluble drug mesoporous silica microparticles based on supercritical fluid technique, Int. J. Pharm. 454 (2013) 135-142.

[47] J.S. Boateng, K.H. Matthews, H.N.E. Stevens, G.M. Eccleston, Wound healing dressings and drug delivery systems: A review, J. Pharm. Sci. 97 (2008) 2892-2923.

[48] V. Falanga, Wound healing and its impairment in the diabetic foot, Lancet. 366 (2005) 1736-1743.

Appendix

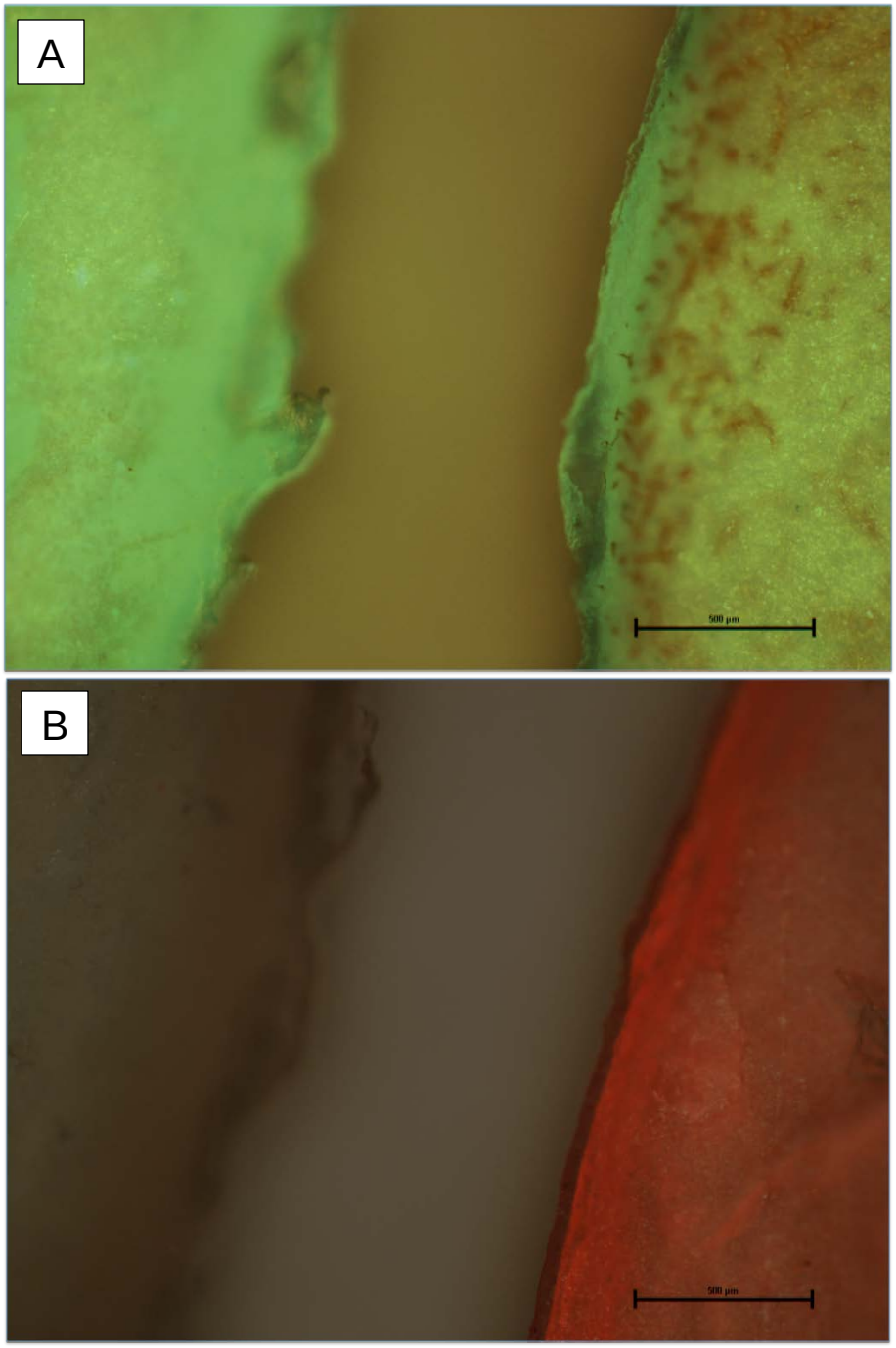

Figure A1: Fluorescence images of dual dye infused (subcritical condition) PCL (left) and PCL-gelatin (right) scaffolds after 14 days of release. A) GFP filter detecting BODIPY B) RFP filter detecting Rhodamine B. One can visibly notice differences in Rhodamine dye fluorescence between PCL (unlike) and PCL-gelatin (like) scaffolds.

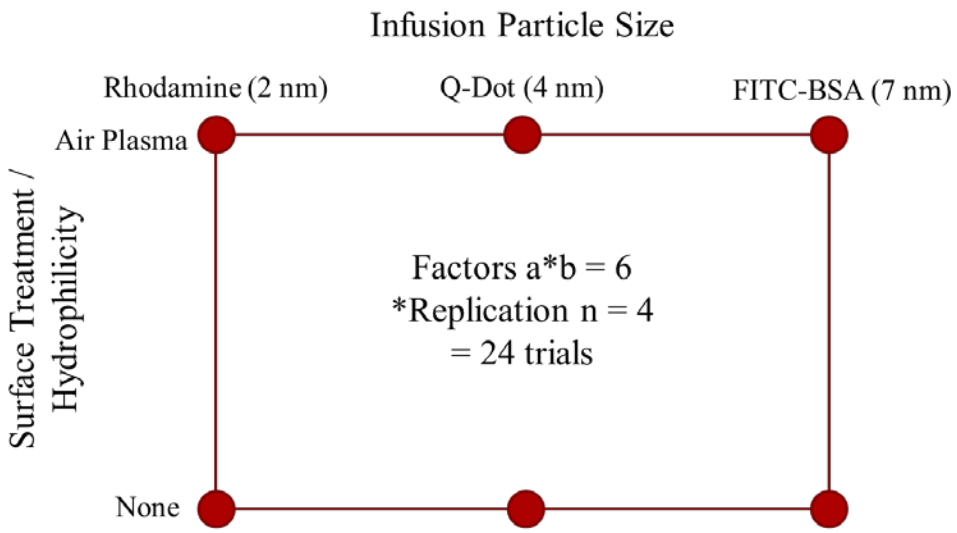

Figure A2: Factorial design to screen factors of particle size, surface hydrophilicity (as induced by plasma treatment and a bit different than material hydrophilicity), and their interaction in future work with CO_2 infused nanofiber systems.

Table A1: Experimental design for the project. Note that supercritical infusion into PCL is not possible; the PCL nanofibers will melt and lose their microstructure. This rendered supercritical infusion into PCL-gelatin less useful, since one could only observe like interactions for Rhodamine B and unlike interactions for BODIPY in the supercritical infusion state. Core-shell design was decided upon after the results in Figures 4 and 5 were analyzed.

BODIPY	adsorption	subcritical	supercritical
PCL	yes	yes	
PCL-gelatin	yes	yes	no
core-shell P-PG	no	yes	yes

Rhodamine	adsorption	subcritical	supercritical
PCL	yes	yes	
PCL-gelatin	yes	yes	no
core-shell P-PG	no	yes	yes

Both	adsorption	subcritical	supercritical
PCL	yes	yes	
PCL-gelatin	yes	yes	no
core-shell P-PG	yes	no	no